Comparison of Electromagnetic and Piezoelectric Energy Harvesting Methods for Intelligent Tyre Systems

Otso Jousimaa

School of Electrical Engineering

Thesis submitted for examination for the degree of Master of Science in Technology.

Espoo XX.XX.XXXX

Thesis supervisor:

Prof. Arto Visala

Thesis advisors:

M.Sc. Yi Xiong

D.Sc. (Tech.) Ari Tuononen

Aalto-yliopisto
Sähkötekniikan korkeakoulu

AALTO UNIVERSITY
SCHOOL OF ELECTRICAL ENGINEERING

ABSTRACT OF THE
MASTER'S THESIS

Author: Otso Jousimaa

Title: Comparison of Electromagnetic and Piezoelectric Energy Harvesting Methods for Intelligent Tyre Systems

Date: XX.XX.XXXX Language: English Number of pages: 6+20

Department of Automation and Systems Technology

Professorship: Smart products

Supervisor: Prof. Arto Visala

Advisors: M.Sc. Yi Xiong, D.Sc. (Tech.) Ari Tuononen

Your abstract in English. Try to keep the abstract short; approximately 100 words should be enough. The abstract explains your research topic, the methods you have used, and the results you obtained. Your abstract in English. Try to keep the abstract short; approximately 100 words should be enough. The abstract explains your research topic, the methods you have used, and the results you obtained.
Your abstract in English. Try to keep the abstract short; approximately 100 words should be enough. The abstract explains your research topic, the methods you have used, and the results you obtained. Your abstract in English. Try to keep the abstract short; approximately 100 words should be enough. The abstract explains your research topic, the methods you have used, and the results you obtained.

Keywords: For keywords choose concepts that are central to your thesis

AALTO-YLIOPISTO
SÄHKÖTEKNIIKAN KORKEAKOULU

DIPLOMITYÖN
TIIVISTELMÄ

Tekijä: Otso Jousimaa

Työn nimi: Energy Harvester Design for Intelligent Tire Systems

Päivämäärä: XX.XX.XXXX Kieli: Englanti Sivumäärä: 6+20

Automaatio- ja systeemitekniikan laitos

Professuuri: Älykkäät tuotteet

Työn valvoja: Prof. Arto Visala

Työn ohjaajat: DI Yi Xiong, TkT Ari Tuononen

Tiivistelmässä on lyhyt selvitys (noin 100 sanaa) kirjoituksen tärkeimmästä sisällöstä: mitä ja miten on tutkittu, sekä mitä tuloksia on saatu. Tiivistelmässä on lyhyt selvitys (noin 100 sanaa) kirjoituksen tärkeimmästä sisällöstä: mitä ja miten on tutkittu, sekä mitä tuloksia on saatu.
Tiivistelmässä on lyhyt selvitys (noin 100 sanaa) kirjoituksen tärkeimmästä sisällöstä: mitä ja miten on tutkittu, sekä mitä tuloksia on saatu. Tiivistelmässä on lyhyt selvitys (noin 100 sanaa) kirjoituksen tärkeimmästä sisällöstä: mitä ja miten on tutkittu, sekä mitä tuloksia on saatu. Tiivistelmässä on lyhyt selvitys (noin 100 sanaa) kirjoituksen tärkeimmästä sisällöstä: mitä ja miten on tutkittu, sekä mitä tuloksia on saatu.

Avainsanat: Vastus, Resistanssi,
Lämpötila

Preface

I want to thank Professor Pirjo Professori and my instructor Olli Ohjaaja for their good and poor guidance.

Otaniemi, 16.1.2015

Eddie E. A. Engineer

Contents

Symbols and abbreviations

Symbols

$\mathbf{A}$	area
$\mathbf{B}$	magnetic flux density
c	speed of light in vacuum $\approx 3 \times 10^8$ [m/s]
ε	electromotive force
$\mathbf{F}$	mechanical force
$\mathbf{I}$	electrical current
$\mathbf{l}$	length
Φ_B	magnetic flux through loop area
ρ	resistivity
$\mathbf{P}$	power
$\mathbf{p}$	pressure
$\mathbf{U}$	input to system
$\mathbf{V}$	voltage
$\mathbf{Y}$	output from system
$\mathbf{Z}$	complex impedance

Operators

$\frac{\mathrm{d}}{\mathrm{d}t}$	derivative with respect to variable t
$\frac{\partial}{\partial t}$	partial derivative with respect to variable t
$\sum_i$	sum over index i

Abbreviations

AC	Alternating Current
BLE	Bluetooth Low Energy
DC	Direct Current
EMF	Electromotive Force
IC	Integrated Circuit
MEMS	Microelectromechanical Systems
MPPT	Maximum Power Point Tracking
PV	Photovoltaic
RF	Radio Frequency
SMPS	Switch-Mode Power Supply
TPMS	Tire Pressure Monitoring Sensors

1 Introduction

As technology advances, it has become possible to build small, light-weight and yet powerful sensor platforms which can communicate wirelessly with their environment. New kind of applications are being created using the possibilities given by these sensor platforms. A common feature with all of these devices is that they need power to function, even if the power needed is minuscule.

Traditionally wireless devices have been powered by batteries, but as the number of sensors increases, the cost of changing or charging batteries becomes significant part of cost of any system. This is especially relevant for the devices which are in hard-to-reach areas, such as inner parts of heavy machinery, walls of bridges and high rise buildings, remote environmental sensors et cetera. On some applications the life of the battery can become a limiting factor for the lifetime of entire sensor, if cost of installing new sensor is similar to cost of replacing the battery.

A new approach to powering the device is to harvest the energy from it's surroundings using ambient energy as the power source. Examples of such energy sources are solar, wind, temperature differentials, and vibration. The technology to utilise some of these power sources, such as wind and solar is already widely deployed and even used in the large-scale power production. On a smaller scale the demand for reliable and efficient solutions has been growing strongly with the advent of wireless low-power devices and a lot of research has focused on creating suitable technologies and devices for low-power energy harvesting.

This work focuses on powering one of such devices, namely a sensor inside a car tyre. The car tyre provides some unique challenges and opportunities, as there is a lot of energy available, but on the other hand operating conditions can be extremely harsh with large temperature ranges and extreme vibration and shocks especially in rougher road conditions.

Car tyre sensing itself has been in focus of a lot development lately, as legislation in the United States demands new tyres being fitted with a pressure sensor to warn drivers about the low pressure and related higher fuel consumption, wear on tyre and even elevated risk of accidents. European Union has also laws which require Tire Pressure Monitoring Sensors (TPMS) on new passenger cars.

This paper is based on my Master's Thesis which is still a work in progress. The next section has overview of car tyres and the operational environment inside them. A quick review on possible energy harvesting technologies is made, piezoelectric and electromagnetic energy harvesting are selected for in depth comparison. Two different approaches are used determining the applicability of energy harvesting method: electromagnetic generator is researched based on theoretical analysis and simulation while piezoelectric harvesting is researched using experimental methods.

Conclusion presents findings based on the theoretical and experimental research phases of the work and discusses future work to be done to validate findings of theoretic designs.

2 Background

2.1 Structure of a tyre

Tyres are composed of several layers with different functions. Figure 1 by Gent et al. [8] shows the layered structure. From outer tread to inner lining, the layers are:

Tread provides traction for driving, braking and cornering. Pattern and materials on tread is a compromise between wear resistance, traction, handling and rolling resistance

Belts provide mechanical strength, impact resistance and keep tyre from expanding under centrifugal forces.

Body ply provides strength to contain the air pressure.

Innerliner is a compound specifically designed to improve air retention in tyre.

In addition there are layers designed to improve tyre reliability, such as the belt wedge which reduces shear between belts.

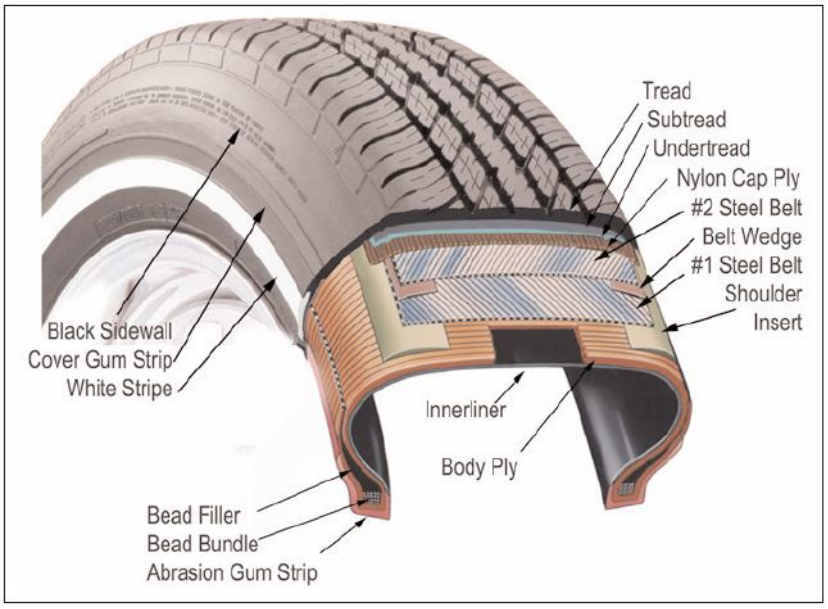

Figure 1: Structure of a tyre [8].

In endurance testing of tyres the car is driven at test track in three shifts until desired number of course driving kilometres have been reached. In outdoor testing each company has their own proprietary test protocol. Indoor testing has standards, which mandates pressure, ambient temperature and speed as well as time driven. According to Gent et al. [8] this indoor testing takes 34 hours of driving at 120 km/h.

In addition to endurance testing, there is high-speed testing where tyre speed is gradually accelerated in steps of 10 km/h at regular intervals until target speed is

reached. Energy harvester should survive these tests to be considered a viable design for road conditions.

2.2 Environment inside tyre

The energy harvester will be placed inside the tyre. Previous studies by Niskanen et al [19]. have shown that the tyre will experience acceleration in all three axes. Tangential and centripetal accelerations are dominant, they can reach amplitudes up to 150 g in test fixture. In addition a study done by Löhndorf et al. [14] shows shock survival of up to 4 000 - 5 000 g is required for reliability.

Temperature inside of the tyre will reach equilibrium in ambient + 5-10 °C, so operation temperature should be in range of -40 to + 75 °C to have some safety margin on top of usual ambient conditions.

Previous work by Niskanen et al. [19] was used to as a basis for analysis of characteristics of acceleration inside the tyre. Raw data was used to gather minimum and maximum values of acceleration as well as frequency components inside tyre. Data was gathered at 20 km/h, 60 km/h and 80 km/h speeds. Figure 3 shows time domain representations of the acceleration along 3 axes as shown in figure 2.

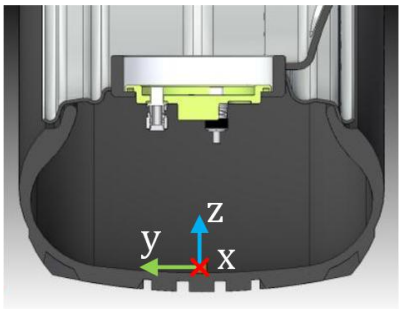

Figure 2: Axes in measurement by Matilainen et al. [16]

Frequency domain representations were calculated in Matlab. There are two main contributors to base frequencies: first is the rotational frequency of tyre itself and second is the impact when the tyre deforms as it contacts the drum.. There is clearly visible series of frequency components spaced at the rotational frequency of tyre as well as shock harmonics at upper frequencies. Figure 4 shows the total frequency spectrum and the dominant frequency components.

It's important to notice that the sensor used was piezoelectric, which forms a highpass filter as the operation of sensor is based on charge between layers. This charge dissipates over time, so the steady-state centripetal acceleration reads as zero. Any device on the rotating tyre will experience centripetal acceleration (acceleration toward centre of rotation) at the amplitude of:

$$a_{centripetal} = \omega^2 r, \tag{1}$$

where ω is the rotation speed of tyre and r is the radius of rotation.

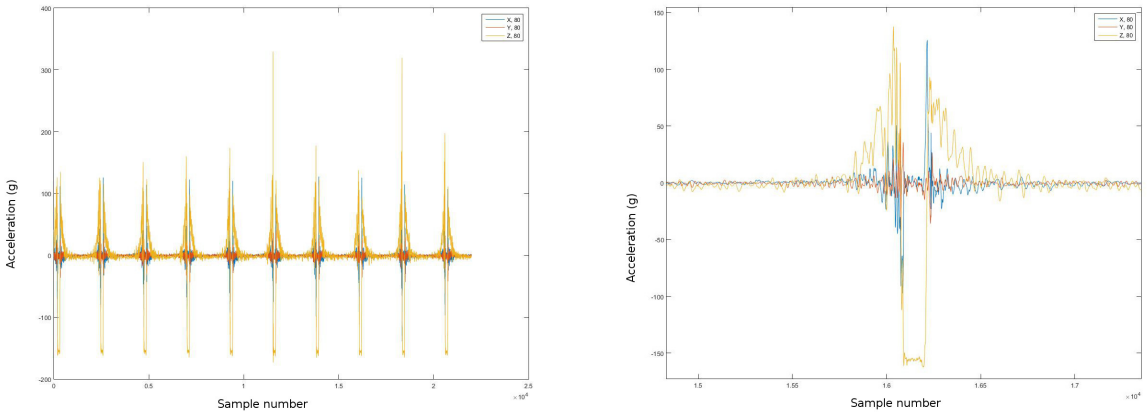

Figure 3: Acceleration of inner lining of tyre at 80 km/h in time domain.

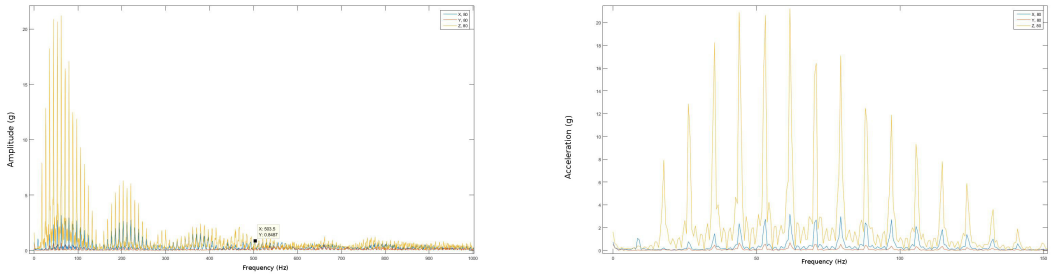

Figure 4: Most of the energy is found in 10-100 Hz range.

3 Energy harvesting

3.1 Overview of methods

First step of designing a system for energy harvesting was to identify the currently known methods and their properties. Kubba et al. [12] have done a study on tyre pressure sensor technology, they present electromagnetic, electrostatic, piezoelectric and thermal solutions as possible candidates for energy harvesting. In addition, triboelectric and magnetostrictive methods have been proposed by Bowen et al [5]. Outside of the context of tyres, Paradiso et al. [21] present solar and radio wave harvesting techniques. Radioactive power source has been suggested by Lal et al [13].

Electromagnetic power sources are based on Faraday's law of electromagnetic induction. A magnet and a coil are put in motion relative to each other, and the changing magnetic flux through the coils of the generator produces voltage. Current through such device is determined by load resistance. Technology is widely used in power generation, where a primary power source such as wind or flow of water provides rotation for the generator. While conventional designs use rotational movement, linear generator designs exist. Boldea and Nasar [4] provide an overview of linear

generator and actuator theory.

Electrostatic devices charge plates of a capacitor and use mechanical vibration to vary the structure of the capacitor. As the capacitance value changes with the structure, energy can be harvested from increased potential energy in capacitor. Drawback of this method is the required control electronics and high polarisation voltages needed for maximal efficiency. There are also electrostatic methods which use electrets. These electrets hold constant charge and polarisation for years and they can be used in electrostatic harvesters which do not require an external excitation source [3]. As electret elements and electrostatic generators are not readily available, they have been excluded from this study.

Piezoelectric materials generate charge in response of mechanical stress. This stress can be caused by firmly attaching the piezoelectric element to a surface which deforms (simply supported) or by leaving one end of the element free-hanging while other end is fixed (cantilevered). Dynamics of the generator are very different for the different configurations, Kim et al. [11] provides a model for impact-based piezoelectric harvester while Erturk et al. have done in-depth analysis of cantilevered piezoelectric modelling [6].

Thermal solutions can be further divided into subcategories. Seebeck-effect where a temperature gradient in a semiconductor material causes voltage between poles of the material is widely used in temperature sensing, but to generate appreciable amounts of power large temperature gradients of over hundred °C are required according to study by Amatya et al. [1]. Such temperature gradients are not practical inside the tyre. Pyroelectric materials do not require differential of temperature, they generate energy when the temperature of the entire element changes [26]. As the temperature inside tyre remains rather constant over long periods of time, these methods are not practical for this application.

Triboelectricity generates power using friction between two materials, a classic example of this is Benjamin Franklin's experiments on charging various rods by rubbing them against different materials. A flexible triboelectric generator has been presented by Fan et al. [7]. Triboelectric sheets are not readily available and their construction is complex, so triboelectric generation is excluded from this work.

Magnetostrictive materials change their magnetic field in response to external mechanical stress. This change can be utilised to create a magnetic flux through coils as in electromagnetic generators. A magnetostrictive generator was built by Wang et al. [24].

Solar energy can be harvested by using sun as a energy source for a thermal energy harvesting or by utilising the photovoltaic (PV) effect to generate electricity from photons hitting PV material. PV technology is mature and widely used, and PV cells attached to rim of tyre could produce ample power during summertime. PV cells would however incur extra maintenance as the rims would have to be cleaned whenever power output falls.

Radio wave harvesting uses antennas to collect energy from ambient radio transmissions, such as WiFi- and cellular signals. Patel et al [22] have built a demonstration device which uses TV broadcasts as an energy source. The tyre material dampens any Radio frequency (RF) broadcasts, which makes RF energy harvesting poorly

suited for the application.

Radioactive energy harvesting resembles battery or fuel cell. A radioactive material is deposited in generator near piezoelectric cantilever. Radioactive decay charges proof mass of piezoelectric cantilever until the proof mass contacts the radioactive material by electrostatic attraction, at which point the electrical charge is balanced and piezoelectric beam begins resonant vibration as in normal piezoelectric harvesting. Such a battery has lifetime limited only by half-life of the used material. Lal and Blanchard [13] present such a battery. This kind of battery would be redundant for the application, as there already exists energy in rotation of tyre which can be used to energise the cantilever.

In conclusion, a wide range of energy harvesting technologies have been identified. As their primary properties are known, we can narrow down the suitable technology to electromagnetic, piezoelectric and magnetostrictive. These technologies are studied further to identify optimal choice for the application.

3.2 Resonance-based piezoelectric harvesting

Piezoelectric materials produce voltage in response to mechanical stress. The effect is bidirectional, piezoelectric element can also produce mechanical strain in response to applied voltage. The material has crystalline structure with electrical dipoles in balanced state when no stress is applied. Mechanical stress unbalances these dipoles, creating element which electronically resembles a charged capacitor.

A common approach to piezoelectric harvesting is to configure the element as a cantilever and tune the resonant frequency of the system to dominant frequency of the surrounding environment. This kind of system is shown in figure 5. In some applications, such as in machines running at the frequency of power grid (50 Hz or 60 Hz) this kind of frequency-tuning is relatively straightforward.

Figure 5: Piezoelectric generator configured as cantilever by Arroyo et al [2].

This kind of resonant harvesting is challenging in tyre. The energy harvester has a very sharp peak efficiency frequencies, and dominant frequency of tyre varies with the speed of car. On the other hand, there is almost guaranteed broadband energy available from moments where tyre contacts road. There is also some research on tuning the resonant frequency of cantilevered piezoelectric harvester by Singh et al [23]. They used intelligently driven SMPS to impedance-match the load to

piezoelectric element. As the electro-mechanical nature of piezo means changing load changes the mechanical properties of element, resonance frequency can track the dominant frequency of system within some limits. Figure 6 shows the tracking behaviour Singh et al achieved, resonance can be adjusted in range of 65 - 70 Hz.

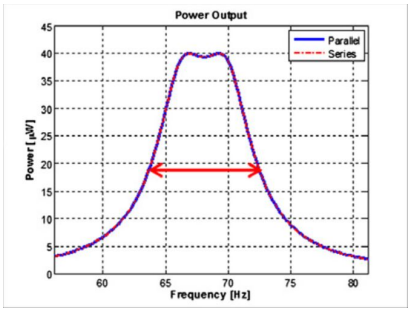

Figure 6: Frequency tuning results by Singh et al [23].

The results of Singh et al. can be considered as the state-of-art for resonance-based piezoelectric harvesting in tyre, and their power output was around $40\mu W$ at peak efficiency. Therefore other methods have to be explored for energy harvester design.

3.3 Impact-based piezoelectric harvesting

As the resonant harvesting is not feasible in the environment inside tyre, another method would be to use an impactor to hit a piezoelectric plate on every cycle of a tyre. These impacts would provide energy once per rotation of a tyre. This method has been tried before by Manla et al [15]. Their generator produced 4 mW electrical power.

As 4mW is plenty in field of low-power electronics, this approach deserves an in-depth study. Thunder TH-5C piezos have been used in previous studies of piezoelectric harvesting and they have produced promising results, so they were selected as the piezoelectric element for this thesis.

piezoelectric elements are often electrically modelled as current source with parallel capacitor or voltage source with series capacitor, as shown in figure 7 by Kanda et al [10]. There are also a lot more complex models which account for mechanical phenomena in piezo, as well as loading effects coupling on mechanical model. For the purposes of model identification for the piezo only simplest voltage source (a) and current source (b) models are explored.

Series of tests were ran to determine characteristics of piezoelectric power generation under impacts. Mossi et al [18] have produced a recommended test process for Thunder piezoelectric actuators shown in figure 8.

This setup was replicated using a solenoid actuator as impact force generator, precision scale as load cell to measure impact force and oscilloscope to view output waveforms. An eraser was cut to shape to act as preload bellow to spread the impact over larger surface area of piezo, displacement was not measured. The test setup is shown in figure 9. An electronics prototyping platform, "breadboard", was used to

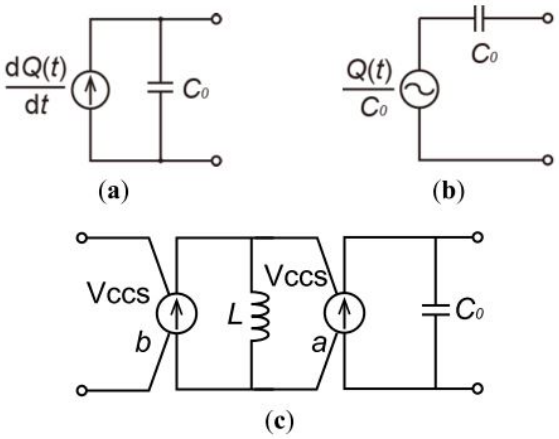

Figure 7: Electrical equivalent models for piezoelectric element [10].

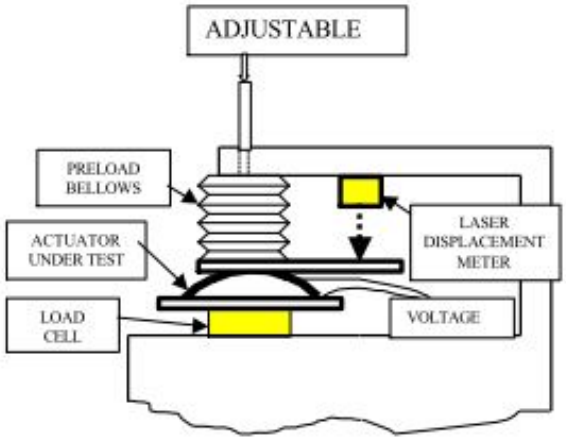

Figure 8: Recommended evaluation platform for Thunder piezos [18].

house test electronics including resistive ladder and Arduino to trigger the solenoid at adjustable duty cycles. Load force was controlled by setting the stroke length of solenoid shaft and fine tuned by adjusting voltage over solenoid.

The measurement results are shown in figure 10. Output voltage scales with square of impact force, which makes sense as work done can be expressed as $W = F * d$, where W is work, F is force and d is distance force acts on object. As the displacement of piezo grows with the applied force, total work and therefore energy grows with both terms.

Peak voltage grows with the load resistance. This makes sense in both voltage source and current source models, as the capacitor starts to discharge through load resistance instantly when voltage is applied over it. The relationship between voltage and load resistance seems to be logarithmic, which would be in good agreement with the logarithmic discharge curve of capacitor-resistor system. Peak voltages were read

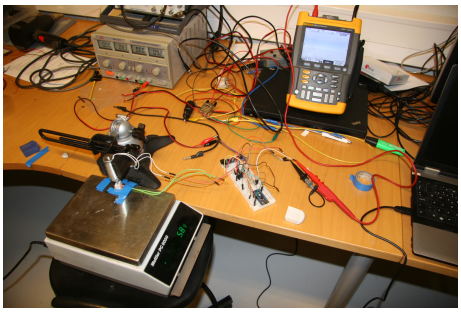

Figure 9: Test platform for piezo characteristics.

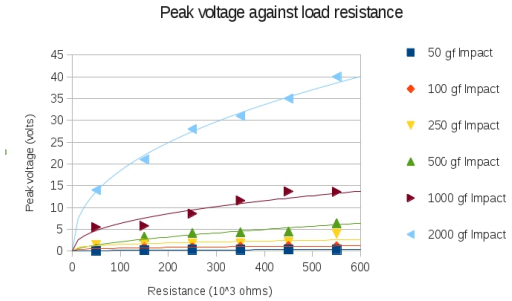

Figure 10: Measured output voltage at different loads and impact forces.

out from digital display and they can be considered reasonably accurate.

The time constants for voltage halving was graphically measured from oscilloscope waveforms, and this data was used to calculate the capacitance of TH-5C. These measurements are a lot less accurate, as readouts from oscilloscope screen have resolution of approximately half of line division, leaving accuracy of measurements at $\pm 2.5ms$. These results are plotted in figure 11

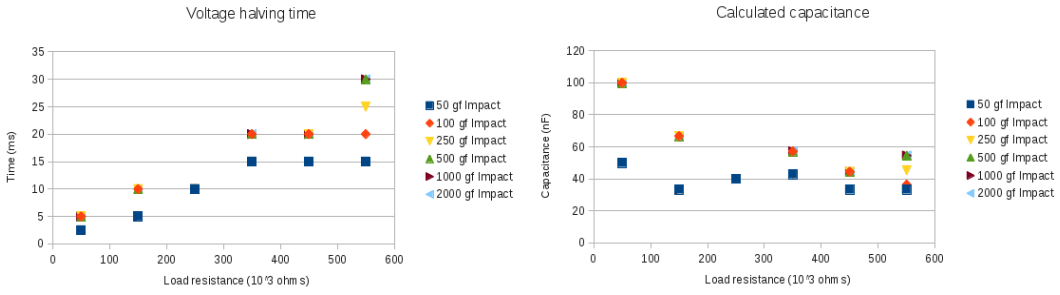

Figure 11: Measured half-time of system and calculated capacitance of piezo.

The half-time data can be used to calculate capacitance of piezo using the RC-time constant of circuit:

$$C = \frac{t}{-ln(\frac{1}{2})R} \tag{2}$$

TH-5C provides value of 39nF as the capacitance, while these calculated values are notably higher and rise with the loading of piezo. Most likely explanation of this observation is the mechanical response time of system: solenoid plunger will take some milliseconds to reach new force equilibrium, and this effect becomes more pronounced at smaller time constants of RC-system. Using the known voltage and capacitance energy and peak power in impact can be determined:

$$E = \frac{1}{2}V^2C \tag{3}$$

$$P_[peak = \frac{V^2}{R} \tag{4}$$

The calculations are plotted in graph 12. As these calculations are based on inaccurately measured time, they should not be used as reference for any further calculations. However, trends can be seen in these values.

Interestingly the peak work done by piezo to resistor seems to be almost constant on all load levels. This is probably a consequence of logarithmic voltage-load relationship described above. There is a possibly significant result based on these findings: total energy obtainable from harvester grows with load resistance. However, this is applicable only for resistive load under impact-based energy generation.

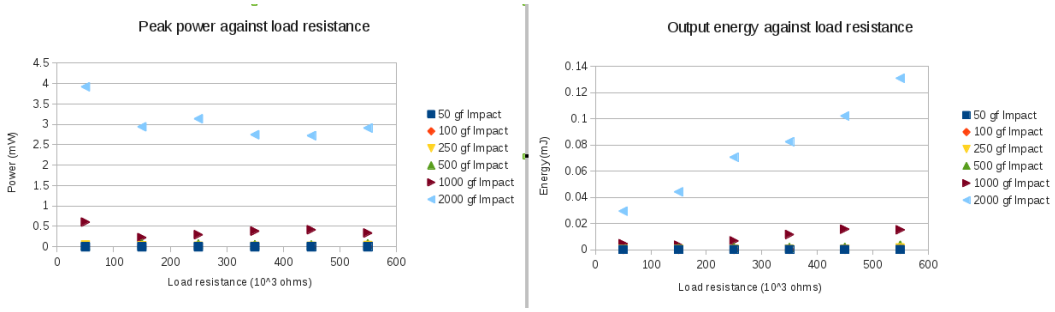

Figure 12: Calculated piezo power and energy output

Based on these results, an electrical equivalent model of circuit was designed. The model is shown in figure 13. Model has two parallel current sources, one to simulate impact of plunger on piezo and other to simulate release of the impact. Capacitance in parallel is set to 39 nF as given in datasheet, load resistance is parametrised to step through the experimental values.

Model was tuned by first calculating the total current transfer to reach the open circuit voltage over capacitor. Then maximum current of current sources was matched to reach peak voltage over highest load. The simulated data is plotted figure 14.

The experimental and simulated data are not in a good agreement. While maximum and minimum load voltage and power are close to estimated values, this is

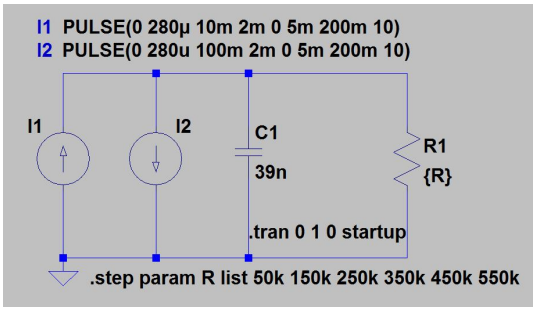

Figure 13: Equivalent model of piezo in LTSpice simulator

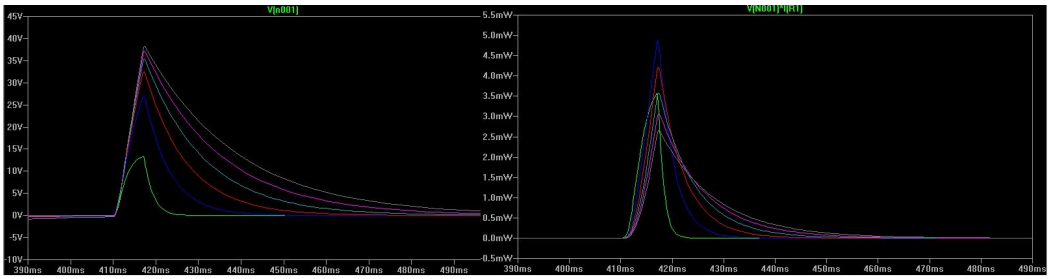

Figure 14: Simulated piezoelement output voltage and power waveforms. Loads are stepped through list to match experimental values at 2000 gf impact force. Green: 50k; Blue: 150k; Red: 250k; Turquoise: 350k; Violet: 450k; Gray: 550k

by design as model is tuned to these measurements. Problems occur in interpolating the results, as output voltages are notably higher than measured values. This provides a result which sets the maximum power load near the value which provides output voltage of half of the open loop voltage. This is especially interesting as LTC3331 datasheet [?] suggests to set the circuit to track the load at this same half-point of open loop voltage. Both LTC3331 and LTSpice are made by Linear Technology, so independent verification of this result would be needed.

3.4 Electromagnetic harvesting

Electromagnetic harvesting is based on Faraday's law of induction: A loop of wire acquires electromotive force (EMF) in response to a changing magnetic field. More formally:

$$\varepsilon = -\frac{d\Phi_B}{dt}, \tag{5}$$

where ε is the EMF, Φ_B is magnetic flux through loop area, and t is time. Negative sign signifies that emf opposes the change of magnetic flux. For a tightly wound coil of wire, the equation can be stated as:

$$\varepsilon = -N_{turns}\frac{d\Phi_B}{dt}, \tag{6}$$

where N_{turns} is the number of turns in a coil. [25, p.999]

It's important to notice that magnetic flux through wire Φ_B can change for a variety of reasons: the source of field can be in motion, strength of field can vary, the coil can be in motion, and the shape of coil can vary. In an energy harvesting application in an environment with vibrations motional energy is readily available, so we focus on energy harvesting methods which either move the source of magnetic field or the coil itself.

It can be determined from equation (6) that the energy available increases with the strength of magnetic source, number of turns in a coil and rate of change in the magnetic field.

Magnetic source can be either a permanent magnet or an electrically induced source as in induction motors. Induction-based generators require reactive power to start up, which means that any harvester design incorporating an induction generator would need a secondary power source to start the inductive generator. Hence the focus of this thesis will be in permanent magnet designs.

In addition to voltage available from the generator, it's important to consider the source impedance. A very simple electrical equivalent model of the generator is presented in figure 15, where generator is presented as a voltage source in series with lumped inductor and resistor [9].

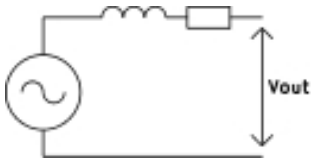

Figure 15: A simple electromechanical generator equivalent circuit.

.

This model is greatly simplified and it does not account for factors such as effect of electromagnetic force on mechanical structure of the generator. Even with these limitations, the model is still useful as it can be used to determine an optimal load for the generator.

The power output can be written formally as:

$$P_{generated}(s) = \varepsilon(s) * I_{generated}(s), \tag{7}$$

where $P_{generated}(s), \varepsilon(s), I_{generated}(s)$ are complex frequency-domain power, voltage and current dependent. Voltage is determined by EMF as described above. Current can be written as:

$$I_{generated}(s) = \frac{\varepsilon(s)}{Z_{generator}(s) + Z_{load}(s)}, \tag{8}$$

where $Z_{generator}(s)$ and $Z_{load}(s)$ are complex impedances of load and generator. This equation is valid only for linear systems, so for example rectifying and converting power with switch-mode power supply (SMPS) reduces accuracy of the equation. Substituting (8) into (7) we obtain:

$$P_{generated}(s) = \varepsilon(s) * \frac{\varepsilon(s)}{Z_{generator}(s) + Z_{load}(s)}. \tag{9}$$

Total power into load can be written as:

$$P_{load}(s) = \varepsilon(s) * \frac{Z_{load}(s)}{Z_{generator}(s) + Z_{load}(s)} * \frac{\varepsilon(s)}{Z_{generator}(s) + Z_{load}(s)}. \tag{10}$$

It's easy to see from (10) that if the load impedance is infinite or zero, there is no power generated. It can be shown that maximum power is generated when load impedance is complex conjugate of generator impedance, $Z_{generator}(s) = Z_{load}(s)^*$. Another consideration is efficiency of the generator: the electrical efficiency is defined as ratio of power flowing into load and total power generated. Equation (10) can be used to show that when load impedance is equal to generator impedance, efficiency is 50%. Efficiency rises with the load impedance, which is why generators are rarely run at their maximum power. In our application the harvested power is minuscule compared to power available in tyre, so it makes sense to try to match the load impedance for maximum power.

In an energy harvesting application it is important to consider the validity of established theory when generator is scaled to centimetres or even smaller dimensions. Many assumptions, such as coil being tightly wound and made of thin wire might become invalid at microscale. O'Donnel et al. [20] have done a study on the effects of scaling dimensions downward down to millimetre range, and they concluded that power available from generator is proportional to fourth power of generator dimension for cubical generators. Another of their primary findings was that a microfabricated generator becomes more effective than a traditional wire-wound generator when design is scaled below $2mm$ length or in $8mm^3$ volume. It can be concluded that in this application it is reasonable to use a wire-wound generator over microfabricated one, as the generator dimensions can be an order of magnitude larger than this crossover point.

As some parameters of the harvester are difficult to solve analytically, these parameters are solved using experimental and FEA methods. First one of these difficult interactions is the magnetic force between rotor magnet and balancing magnets. A magnetics FEA software FEMM [17] was used to create an axisymmetric model of magnets in generator. Figure 16 shows the used model. Model has two biasing magnets made of N40-neodymium alloy configured to repel an identical rotor magnet. Magnets have height of 2.5 mm and diameter of 11 mm, walls of generator are modelled as air. Generator has total height of 25 mm, leaving rotor magnet 17.5 mm room for movement inside generator.

Weighted stress tensor integration over rotor magnet volume as implemented by FEMM was used to determine FEA value for net magnetic force acting on rotor magnet. A LUA script was used to move the rotor magnet from bottom of the

generator to top in 0.1 mm increments and values obtained from analysis were exported as CSV data for plotting in a spreadsheet software as well as to create a lookup-table for MATLAB/SIMULINK simulation. Figure 16 shows the force on magnet, positive force meaning force toward the upper magnet and zero height being at the bottom of cylinder. For reference the centrifugal force acting on magnet was also calculated at various speeds, assuming weight of the magnet is 1,67 g and tyre radius to bottom of generator is 275 mm.

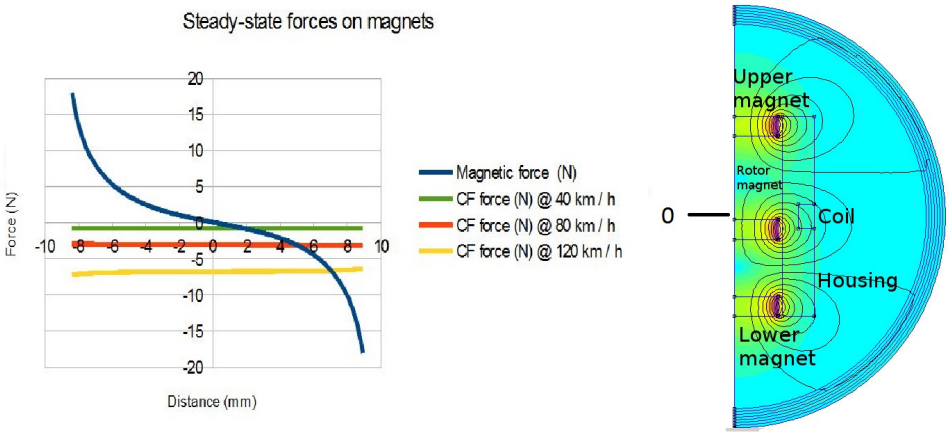

Figure 16: Steady-state forces acting on magnet

These results were used to generate look-up tables for Simulink model shown in figure 17. The model accounts for magnetic, electromagnetic, frictional and pneumatic forces acting on generator. A chirp signal with amplitude of tens of g's was given as an input to model to study the output voltage amplitudes, frequency response and waveforms. The simulated output frequency response (frequency growing from 10 to 500 Hz) and waveforms at low frequencies are shown in figure 18.

A prototype generator was built to test the concept feasibility and identify any practical issues in the generator construction. Generator was machined out of 21mm diameter nylon tubing with 12 mm inner diameter. A groove was machined on the outer diameter to hold the coiling in place. Inner diameter of the groove was 14 mm and height 3 mm. 0.1 mm diameter wire was used to build the coil. To determine the number of turns in coil, coil resistance was measured to determine the length of wire and number of turn was calculated using known length of loop turn and total length of wire. Coil resistance was 42 ohms as the resistance of wire is approximately 2.2 ohms / meter the total length is approximately 19 meters. As one loop has length of 44 mm, coil had roughly 400 turns.

The prototype was connected on a Brüel Kjær shaker type 4905 and driven using Brüel Kjær power amplifier type 2707. Input signal was generated using NI-USB6218 DAQ and output was measured directly from leads of the generator. Vertical displacement of generator was limited to $7.5mm$. Output signal was a sine wave with amplitude of 5 volts, which was amplified by gain of 8 above frequencies of 30 Hz. At lower frequencies the gain was limited to stay within allowed displacement.

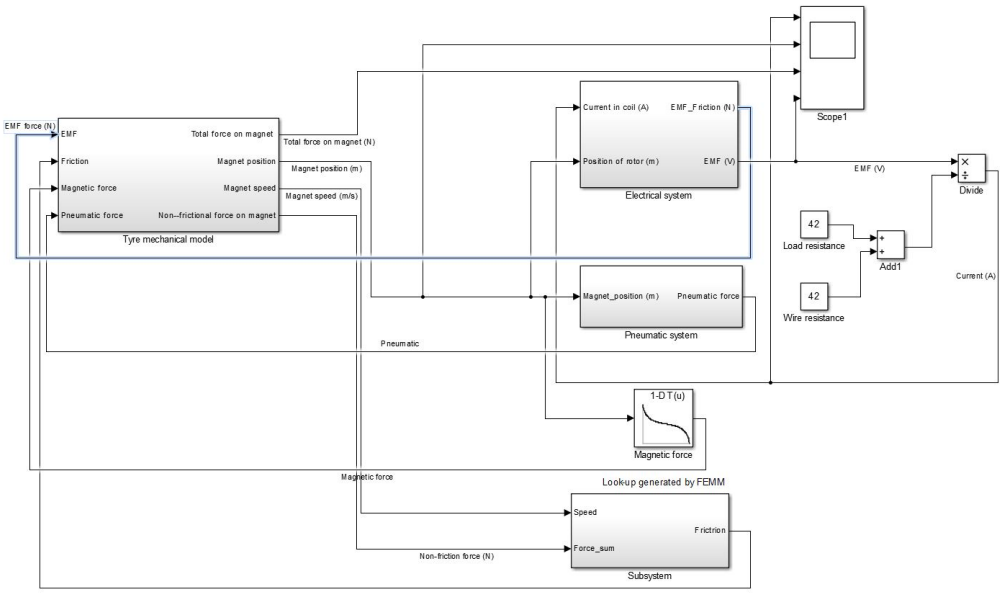

Figure 17: Simulink model of system

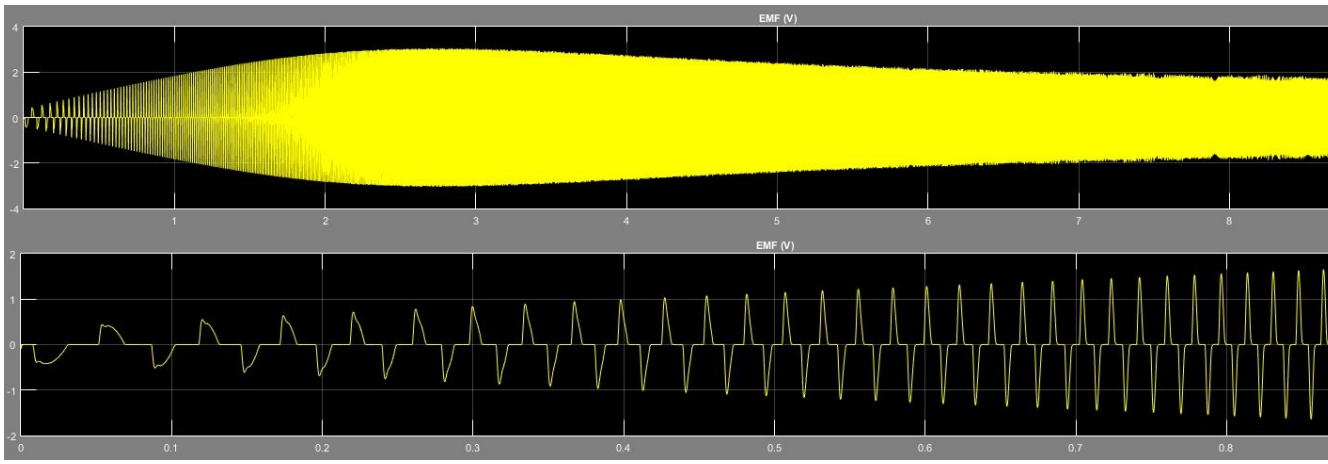

Figure 18: Waveforms of system

Measured graphs are shown in figure 19.

While waveforms are similar in experimental setup as they are in simulation, amplitude of measured signal is order of magnitude lower. Further work is required to determine the source of this discrepancy.

As the coil resistance of prototype generator was measured to be 42Ω, we can predict the theoretical maximum peak power into optimised load to be

$$P = \frac{1}{2}\frac{U^2}{2 * R_{generator}} \approx 130\mu W. \tag{11}$$

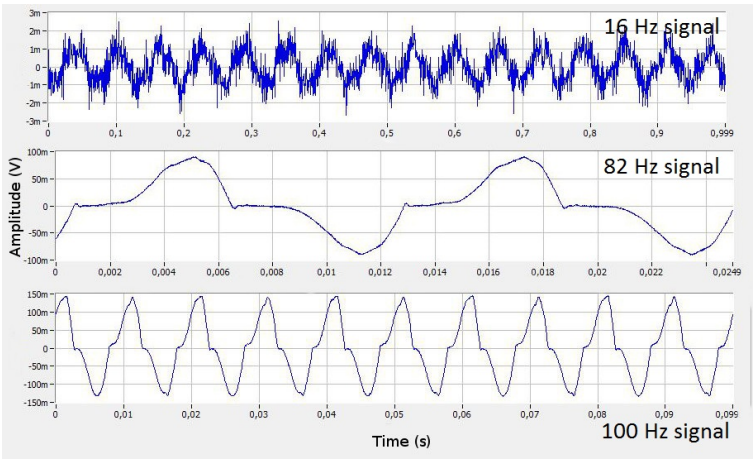

Figure 19: Measured open-loop voltage outputs at various frequencies

4 Conclusions

In this paper the operation environment of tyre has been presented, and reasonable choices for energy harvesting technology have been identified. Both Piezoelectric and electromagnetic methods have been researched. While both methods can produce similar AC-power levels to resistive load, electromagnetic harvesting was found to produce too low voltage for rectification and operation of microcontroller.

Various voltage doubling and active rectification schemes do exist, as well as boost converters and charge pumps which could be used to bring voltage from electromagnetic harvesting to usable levels. However, piezoelectric harvester does not require such extra complexity.

Future work is needed on determining which factors limit the voltage output of electromagnetic harvester below the simulated results as well as to create maximum power point tracking for both methods. In addition, identical test setups will be created to compare the power output of final electromagnetic and piezoelectric generator power levels.

References

[1] R. Amatya and R. J. Ram. Solar thermoelectric generator for micropower applications. *Journal of Electronic Materials*, 39(9):1735–1740, 2010.

[2] E. Arroyo, a. Badel, F. Formosa, Y. Wu, and J. Qiu. Comparison of electromagnetic and piezoelectric vibration energy harvesters: Model and experiments. *Sensors and Actuators, A: Physical*, 183(June):148–156, 2012.

[3] S Boisseau, G Despesse, and B Ahmed Seddik. Electrostatic Conversion for Vibration Energy Harvesting. *Small-Scale Energy Harvesting*, pages 1–39, 2012.

[4] I. Boldea and S. a. Nasar. Linear electric actuators and generators. *IEEE Transactions on Energy Conversion*, 14(3):712–717, 1999.

[5] C. R. Bowen and M. H. Arafa. Energy Harvesting Technologies for Tire Pressure Monitoring Systems. *Advanced Energy Materials*, pages n/a–n/a, 2014.

[6] Alper Erturk, Daniel J Inman, Scott L Hendricks, Michael W Hyer, and Ishwar K Puri. Electromechanical Modeling of Piezoelectric Energy Harvesters. *Health San Francisco*, 2009.

[7] Feng Ru Fan, Zhong Qun Tian, and Zhong Lin Wang. Flexible triboelectric generator. *Nano Energy*, 1(2):328–334, 2012.

[8] a N Gent and J D Walter. The Pneumatic Tire. *Rubber World*, (February):707, 2005.

[9] Panida Jirutitijaroen. EE2022 Electrical Energy Systems Lecture 10 : Electric Power Generation – an Equivalent Circuit of a Generator. 2012.

[10] Kensuke Kanda, Takashi Saito, Yuki Iga, Kohei Higuchi, and Kazusuke Maenaka. Influence of parasitic capacitance on output voltage for series-connected thin-film piezoelectric devices. *Sensors (Switzerland)*, 12(12):16673–16684, 2012.

[11] S H Kim, S Ju, C H Ji, and S J Lee. Equivalent circuit model of an impact-based piezoelectric energy harvester. *Journal of Physics: Conference Series*, 557:012094, 2014.

[12] Ali E. Kubba and Kyle Jiang. A comprehensive study on technologies of tyre monitoring systems and possible energy solutions. *Sensors (Switzerland)*, 14(6):10306–10345, 2014.

[13] B Y Amit Lal and James Blanchard. The daintiest of dynamos. *IEEE Spectrum*, (September):36–41, 2004.

[14] M Löhndorf, T Kvisterø y, E. Westby, and E Halvorsen. Evaluation of Energy Harvesting Concepts for Tire Pressure Monitoring Systems. *International Workshops on Micro and Nanotechnology for Power Generation and Energy Conversion Applications*, pages 331–334, 2007.

[15] G Manla, N.M White, and J Tudor. Harvesting energy from vehicle wheels. *Solid-State Sensors, Actuators and Microsystems Conference, 2009.*, 2009.

[16] Mika J Matilainen and Ari Juhani Tuononen. Intelligent Tire to Measure Contact Length in Dry Asphalt and Wet Concrete Conditions. *Avec 12*, pages 1–6, 2012.

[17] David Meeker. Finite Element Method Magnetics, Version 4.2, 2013.

[18] K M Mossi, R P Bishop, R C Smith, and H T Banks. Evaluation Criteria for THUNDER Actuators 2 . Typical THUNDER Configurations. pages 1–6.

[19] Arto J. Niskanen and Ari J. Tuononen. Three 3-axis accelerometers fixed inside the tyre for studying contact patch deformations in wet conditions. *Vehicle System Dynamics*, 52(sup1):287–298, 2014.

[20] T O'Donnell, Chitta Saha, Steve Beeby, and John Tudor. Scaling effects for electromagnetic vibrational power generators. *Microsystem Technologies*, (April):26–28, 2007.

[21] Joseph a. Paradiso and Thad Starner. Energy scavenging for mobile and wireless electronics. *IEEE Pervasive Computing*, 4(1):18–27, 2005.

[22] Deep Patel, Rohan Mehta, Rhythm Patwa, Sahil Thapar, and Shivani Chopra. RF Energy Harvesting. *International Journal of Engineering Trends and Technology (IJETT)*, 16(8):382–385, 2014.

[23] Kanwar Bharat Singh, Vishwas Bedekar, Saied Taheri, and Shashank Priya. Piezoelectric vibration energy harvesting system with an adaptive frequency tuning mechanism for intelligent tires. *Mechatronics*, 22(7):970–988, 2012.

[24] L Wang and F-G Yuan. Structural Vibration Energy Harvesting by Magnetostrictive Materials (MsM). *4th China-Japan-US Symposium on Structural Control and Monitoring*, pages 1–8, 2006.

[25] Hugh D. Young and Roger A. Freedman. *University Physics*. Pearson, 12th edition, 2008.

[26] Qi Zhang, Amen Agbossou, Zhihua Feng, and Mathieu Cosnier. Solar micro-energy harvesting with pyroelectric effect and wind flow. *Sensors and Actuators, A: Physical*, 168(2):335–342, 2011.